Nexus of Future Materials
https://nfmjournal.com/

Optical Modifications in Eu_2O_3 - Doped Borate Glasses: Impact on Bandgap, Metallicity, and Photonic Properties

Shrikant Biradar [a, b,*], Ashok Dinkar [a], G. B. Devidas [a,*]

[a]Department of Physics, Kuvempu University, Shankaraghatta, Shimoga, Karnataka, India, 577 451
[b]Department of Physics, SSS Government First Grade College, Mudalagi, Karnataka, India, 591 312

Keywords:

Optical Band Gap
Urbach Energy
Refractive Index
Mott and Davis Formula.

Abstract

This study examines the optical properties of (45-x) B_2O_3-6PbO-18ZnO-31Bi_2O_3–xEu_2O_3 glasses (x = 1, 2, 3, and 4 mol%), synthesized using the melt-quenching method. UV-Visible spectra exhibit characteristic absorption peaks of Eu_2O_3, with intensities increasing proportionally to the Eu_2O_3 content. Optical analysis reveals a decrease in the direct energy band gap (E_g) from 2.906 eV to 2.623 eV in the Eu1 to Eu2 samples, attributed to an increase in non-bridging oxygens (NBOs). Conversely, an increase in E_g values from 2.795 eV to 2.842 eV in the Eu3 to Eu4 samples suggests structural densification. The Urbach energy (EU) increases from 0.176 eV to 0.520 eV in the Eu1 to Eu2 samples, while it decreases from 0.222 eV to 0.165 eV in the Eu3 to Eu4 samples. Trends in the refractive index reflect the influence of non-bridging oxygens (NBOs) and bridging oxygen (BO) ratios on the glass network. The dielectric constant (ε), molar refractivity (R_{Molar}), and polarizability (α_{Molar}) correlate with variations in Eu_2O_3 content. A reduction in metallization values from 0.370 to 0.319 indicates increased metallicity from Eu1 to Eu2, while an increase in metallization values from 0.358 to 0.365 for Eu3 and Eu4 suggests a shift toward a more non-metallic nature, consistent with the observed bandgap widening. These findings underscore the intricate relationship between glass structure and optical behavior, paving the way for potential applications in optoelectronic materials.

1. Introduction

In modern technology, glass plays a pivotal role due to its durability and versatile properties. In the construction industry, windows, partitions, and doors are often made from glass, allowing natural light to enter while helping to maintain energy efficiency. Many household appliances use glass to enhance functionality and durability, ranging from decorative items and furniture to cooking materials. Glass materials are highly valuable in communication and technical industries, being used to produce fiber optic cables and screens for electronic devices such as computers and televisions. Glassware is recyclable, sustainable, and eco-friendly. It is chemically and thermally stable with excellent transparency, making it indispensable for chemical and pharmaceutical laboratory equipment as well as solar devices. These properties enhance convenience and safety in everyday activities [1-4].

Due to its importance, glass is widely used in the construction industry and renewable energy sectors. It is essential for the production of windows, facades, and skylights, contributing to energy efficiency, aesthetics, and natural lighting. Unique glass materials are essential for smartphones, optical devices, and computers, playing a critical role in connectivity and innovation. Due to the importance of glass, energy transformation industries rely on it for the production of wind turbines and solar panels. Moreover, due to its inertness and transparency, glass is widely used in the production of test tubes, beakers, radiation shielding materials, and medical tools. Industries such as automotive and aerospace use glass for safety, aerodynamics, and visibility. These unique properties of glass make it an essential material for various applications [5-9]. Due to the diverse chemical compositions used in glass production, numerous glass apparatuses are designed for a wide range of purposes. By partially substituting oxides such as silica, boron, or alkali metals, glasses can acquire unique thermal, optical, and mechanical properties e.g. Borosilicate glasses can withstand thermal shock, making them ideal for laboratory and cookware applications. In contrast, lead glasses enhance refractive properties, which are essential for optical devices and radiation protection.

* Corresponding author:
E-mail address: shreekantsbiradar@gmail.com (S. Biradar), devidasgb02@gmail.com (G. B. Devidas)

Received 12 December 2024; Accepted 24 December 2024;
Published 25 December 2024
https://doi.org/10.70128/588347

Sodium and calcium compounds enhance the durability of commonly used glassware, while specific compositions are critical for energy generation in solar panels and construction applications. Certain modifiable glasses are used in devices like scratch-resistant screens, optical fibers, and bioactive medical implants, supporting applications in communication and healthcare. These modifications enable glass to meet various environmental and industrial demands, enhancing functionality, sustainability, and cost efficiency in production [10-14].

Glass materials composed of B_2O_3, PbO, ZnO, BaO, and Bi_2O_3 offer significant advantages due to their unique properties. B2O3 enhances the thermal and chemical stability of glass, providing resistance to heat shock and making it suitable for various technological applications [15-17]. The presence of PbO (lead oxide) significantly enhances the density and refractive index of a material, playing a crucial role in improving optical transparency. This makes it highly desirable for applications such as lens devices and gamma radiation shielding. [18]. ZnO (zinc oxide) significantly enhances the mechanical properties of glass and provides strong protection against UV rays, minimizing UV damage and increasing the durability of the resulting glass [19-20]. The presence of Bi2O3 (bismuth oxide) in a glass system increases the effective atomic number of the composite, thereby enhancing its density and properties such as optical integrity. These improvements make it an excellent candidate for photon and radiation shielding applications [21-22]. Glass with the aforementioned chemical compositions outperforms conventional glass materials in terms of optical, thermal, radiation protection, and mechanical properties, making it highly desirable for industrial applications. The presence of Eu2O3 (europium oxide) in the B2O3-PbO-ZnO-Bi2O3 glass system gradually enhances its optical integrity due to its photoluminescent properties, making the resulting glass highly suitable for optoelectronic and laser applications. Eu^{3+} and Eu^{2+} are the two oxidation states of europium that play a key role in distinctly enhancing the optical properties of materials. Under UV excitation, Eu^{3+} ions emit red light, making them ideal for display technologies and phosphor applications. Eu^{3+} ions are key contributors to improving light absorption and enhancing luminescence. This study is significant as it reveals the impact of europium doping on the structural and optical properties of lead borate glasses, facilitating precise modulation of key parameters such as the bandgap, refractive index, and polarizability. These insights contribute to the development of customized optoelectronic materials for innovative applications in photonics, sensors, and energy-efficient technologies. This study investigates the optical properties of europium-doped lead borate glasses enriched with zinc and bismuth oxides. It provides essential insights into the correlation between europium concentration, glass structure, and optical behavior, enabling precise tuning of the energy gap and refractive indices. These advancements contribute to the development of advanced optoelectronic materials for applications in detectors and photonic systems.

2. Materials and methods

The glasses in this study were prepared using the melt-quenching method, with their chemical compositions listed in Table 1.

Table 1: Glass codes and chemical composition of the prepared glasses.

Glass Code	B_2O_3	PbO	ZnO	Bi_2O_3	Eu_2O_3
Eu1	44	6	18	31	1
Eu2	43	6	18	31	2
Eu3	42	6	18	31	3
Eu4	41	6	18	31	4

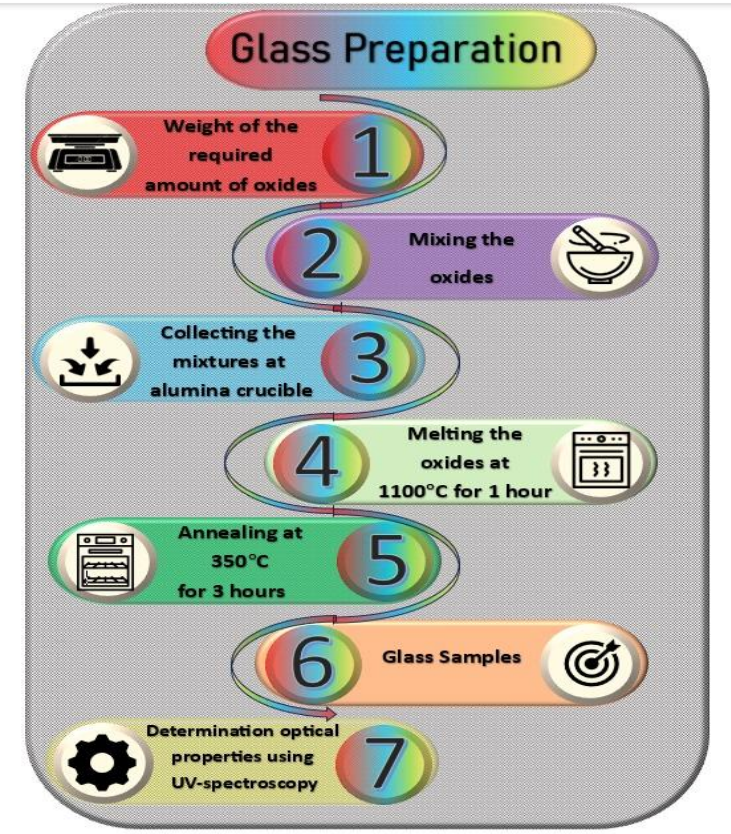

Fig.1. Schematic illustration of the preparation steps for the investigated glasses.

Fig.1 summarizes the steps involved in the preparation of the investigated glasses. The optical properties of the prepared glasses were studied using a double-beam T-7200 UV–Vis spectrophotometer, which recorded the UV–Vis absorption spectra over a wavelength range of 190–1100 nm. The energy band gap (E_g) of the glasses can be calculated using the absorption data by applying the Mott and Davis formula [23-24]:

$$\alpha h\nu = C\left(h\nu - E_g\right)^m \quad (1)$$

here, C is constant, E_g represents the energy band gap, and hν denotes the photon energy. The index m characterizes the type of optical transition (m=1/2 for direct and m=2 for indirect transitions). α is the absorption coefficient, which is calculated using the expression:

$$\alpha = \frac{2.303 \text{ x } A}{t} \quad (2)$$

here, A represents the absorbance and t denotes the glass thickness. The Urbach energy (E_U) provides insight into the structural disorder in the glass and is calculated using the following relation [25]:

$$\alpha = B\exp\left(\frac{h\nu}{E_U}\right) \quad (3)$$

here, B is constant. The following formula can be used to calculate the refractive index (n).

$$\frac{(n^2-1)}{(n^2+2)} = 1 - \sqrt{\frac{E_g}{20}} \quad (4)$$

The dielectric constant (ε) is determined using the refractive index (n) as follows.

$$\varepsilon = n^2 \quad (5)$$

The reflection loss (R_{Loss}) is calculated using the following formula [26]:

$$R_{Loss} = \left(\frac{n-1}{n+2}\right)^2 \quad (6)$$

Optical transmission (T_{opt}) calculated using the following expression:

$$T_{opt} = \frac{2n}{n^2+1} \quad (7)$$

Molar refractivity (R_{Molar}) calculated using the following formula [27]:

$$R_{Molar} = \left(\frac{n^2-1}{n^2+2}\right)V_M \quad (8)$$

Molar polarizability (α_{Molar}) can be evaluated using the following expression:

$$\alpha_{Molar} = \frac{3}{4\pi N_A}R_{Molar} = \frac{R_{Molar}}{2.52} \quad (9)$$

Metallization (M) indicates whether a material behaves as a metal or a non-metal and is calculated using the following equation:

$$M = 1 - \frac{R_{Molar}}{V_M} \quad (10)$$

3. Result and discussion

Fig.2 illustrates the UV-Visible absorption spectra of the Eu1, Eu2, Eu3, and Eu4 glass samples. The purpose of **Fig.2** is to highlight the absorption peaks corresponding to the optical transitions of Eu_2O_3, highlights four distinct absorption peaks within the depicted range. The electronic transitions originate from the lowest state (ground state) $^7F_0$ and progress toward higher energy levels. The absorption bands observed at wavelengths of 464 nm, 524 nm, 534 nm, and 581 nm correspond to electronic transitions from the ground state $^7F_0$ to the excited states $^5D_2$, $^5D_1$, $^5D_1$, and $^5D_0$ respectively [28].

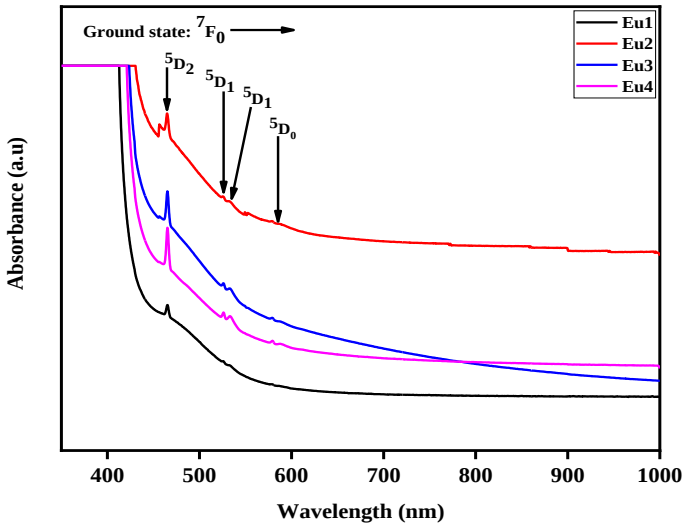

Fig.2. UV-Vis. Absorbance spectra of Eu1, Eu2, Eu3 and Eu4 glasses.

The positions of the absorption peaks remain constant with varying Eu^{3+} ion concentrations, while the absorption intensity increases progressively with higher Eu_2O_3 content. This behavior is attributed to the consistent electronic transitions of Eu^{3+} ions within the glass matrix. Certain rare-earth (RE) ion transitions, known as hypersensitive transitions, are particularly sensitive to their local structural environment, resulting in variations in intensity. Among the transitions observed in this study, the $^7F_0 \rightarrow {}^5D_2$ transition exhibits significantly higher intensity compared to others, highlighting its sensitivity to the surrounding glass network. Previous research has consistently identified most of the prominent absorption bands of rare-earth ions within the visible spectrum [28–29], further supporting these observations. This underscores the significance of structural and compositional factors in tailoring the optical properties of rare-earth-doped materials.

The optical bandgap (E_g) is a crucial parameter in optical studies, serving as a basis for calculating other related quantities. E_g is determined using Equation (1) by plotting $(\alpha h\nu)^m$ versus hν and extrapolating the linear segment to the point where $(\alpha h\nu)^2 = 0$ for direct transitions (E_g^{direct}) and $(\alpha h\nu)^{1/2} = 0$ for indirect transitions ($E_g^{indirect}$), as shown in **Figs. 3** and **4**, respectively.

The observed reduction in E_g^{Direct} values from 2.906 to 2.623 eV and $E_g^{Indirect}$ values from 2.752 to 2.035 eV for the Eu1 to Eu2 samples with increasing Eu_2O_3 content, can be attributed to structural modifications, specifically an increase in the number of non-bridging oxygens (NBOs) [30]. Conversely, the increase in E_g values for the Eu3 to Eu4 samples, from 2.795 to 2.842 eV (E_g^{direct}) and 2.571 to 2.661 eV $E_g^{Indirect}$ respectively, can be attributed to the reduced extent of electron localization and donor centers. These changes arise from modifications in the glass network, leading to a decrease in the number of non-bridging oxygens (NBOs). The shift of the absorption peak to higher energy is associated with the formation of fewer NBOs, resulting in a denser and more compact glass structure [23, 30].

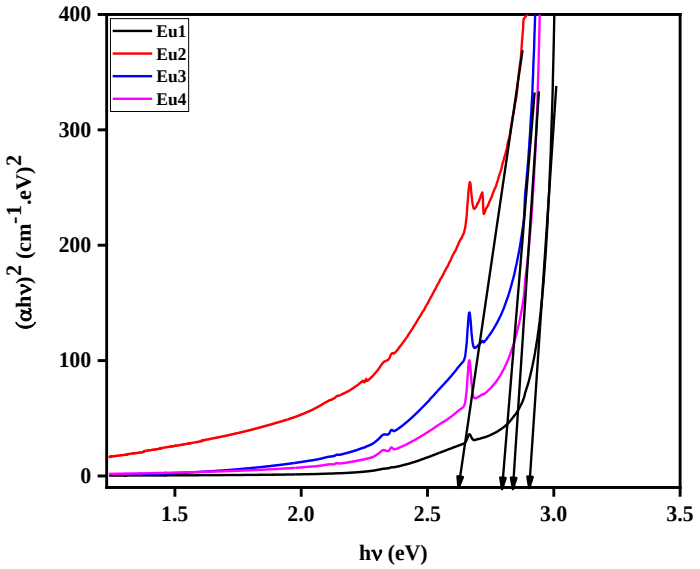

Fig.3. Variation of $(\alpha h\nu)^2$ with hν for the prepared glasses.

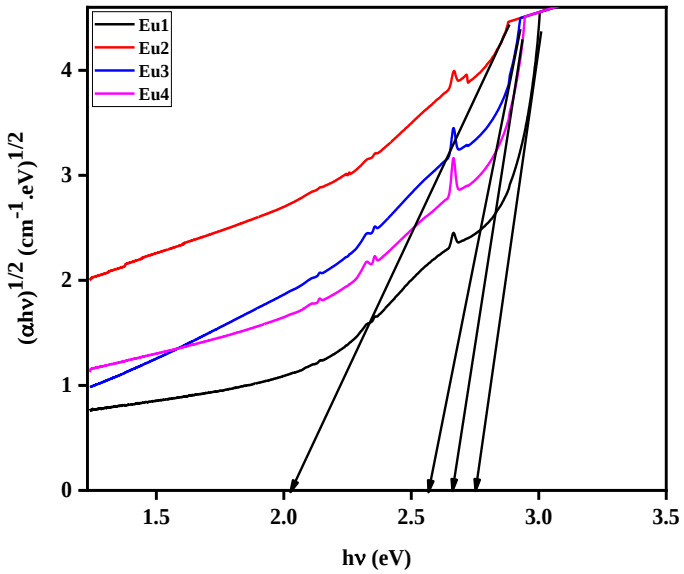

Fig.4. Variation of $(\alpha h\nu)^{1/2}$ with hν for the prepared glasses.

The E_g^{Direct} and $E_g^{Indirect}$ values are presented in Table 2. **Fig.5** shows the Urbach chart, depicting the relationship between lnα and hν for the fabricated glasses. The Urbach energy E_U can be calculated using Equation (3) by determining the inverse slope of the linear section where it intersects the X-axis. As shown in Table 2, the EU values increase from 0.176 eV to 0.520 eV for the Eu1 to Eu2 glasses, respectively. This variation is attributed to the formation of additional defects and an increase in non-bridging oxygens (NBOs) within the glass system, indicating reduced structural rigidity. In contrast, the E_U values for the Eu3 and Eu4 glasses are 0.222 eV and 0.165 eV, respectively, indicating a reduction in defects and, a corresponding decrease in the number of non-bridging oxygens (NBOs) [24–25].

A gradual increase in the refractive index (n) values, calculated using Equation (4) and listed in Table 2, is observed for the Eu1 to Eu2 glasses, however a decrease is noted for the Eu3 and Eu4 glasses as the Eu_2O_3 content increases. The increase in n values is likely attributed to the rise in the number of non-bridging oxygens (NBOs) within the glass structure, while the decrease in n values may be associated with the substitution of B_2O_3 by Eu_2O_3, which exhibits higher polarizability. NBOs form additional ionic bonds, which exhibit higher polarizability compared to the covalent bonds of bridging oxygens (BO). Consequently, as the number of NBOs decreases and BOs increases, the refractive index (n) declines. The increase in Eu_2O_3 content within the glass structure appears to promote the formation of more BOs than NBOs, as reflected in the downward trend in n. The dielectric constant (ε), calculated using equation (5), increases from 6.101 to 7.404 as the Eu_2O_3 content rises from 1 to 2 mol%. This increase in ε is associated with the rise in n values, indicating a reduction in the quantity of bridging oxygens (BOs). However, ε decreases for the Eu3 and Eu4 glasses, attributed to a reduction in the number of non-bridging oxygens (NBOs) [26]. Additionally, other optical properties, including reflection loss (R_{Loss}), optical transmission (T_{opt}), molar refractivity (R_{Molar}), and molar polarizability (α_{Molar}), can be calculated from the n values using Equations (6), (7), (8) and (9), respectively. The corresponding values are presented in **Table 2**. An increase in R_{Molar} and α_{Molar} was observed with the rise in Eu_2O_3 content within the glass system, indicating an increase in the number of non-bridging oxygens (NBOs) in the glass matrix. However, for the glasses Eu3 and Eu4 glasses, the values of R_{Molar} and α_{Molar} decreased due to a reduction in the number of NBOs [24].

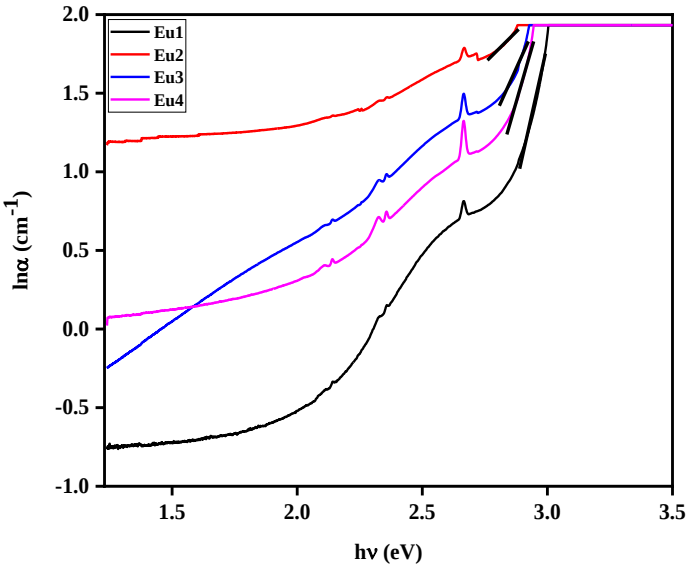

Fig.5. Variation of lnα with hν for the prepared glasses.

Moreover, optical transmission (T_{opt}) decreased for the Eu1 to Eu2 glasses and increased for the Eu3 and Eu4 samples. The variation of R_{Loss} and T_{opt} with Eu_2O_3 content is shown in **Fig.6**. Additionally, the incorporation of Eu_2O_3 leads to a decrease in metallization (M) values, calculated using Equation (10) and presented in Table 2, from 0.370 to 0.319 for the Eu1 to Eu2 glasses. This suggests a reduction in the glass's non-metallic characteristics and a corresponding increase in its metallic properties [26, 28]. However, the Eu3 and Eu4 samples exhibited M values of 0.358 and 0.365, respectively, indicating a reduction in the metallic nature of the glasses. The gradual shift away from metallization also suggests that the conduction band is narrowing, as reflected by the widening optical bandgap.

Table 2: Optical properties of Eu1, Eu2, Eu3 and Eu4 glasses.

Properties	Glasses			
	Eu1	Eu2	Eu3	Eu4
Cut-off wavelength (nm)	437	489	462	449
Direct band gap (eV)	2.906	2.623	2.795	2.842
Indirect band gap (eV)	2.752	2.035	2.571	2.661
Urbach energy, E_U (eV)	0.176	0.520	0.222	0.165
Refractive index, n	2.470	2.721	2.525	2.494
Dielectric constant, ε	6.101	7.404	6.376	6.220
Reflection loss, R_{Loss}	0.179	0.214	0.187	0.183
Optical transmission, T_{opt}	0.696	0.647	0.685	0.691
Molar refraction, R_{Molar} (cm^3/mol)	23.670	25.720	24.348	24.199
Molar polarizability, α_{Molar}	9.393	10.206	9.662	9.603
Metallization criteria, M	0.370	0.319	0.358	0.365

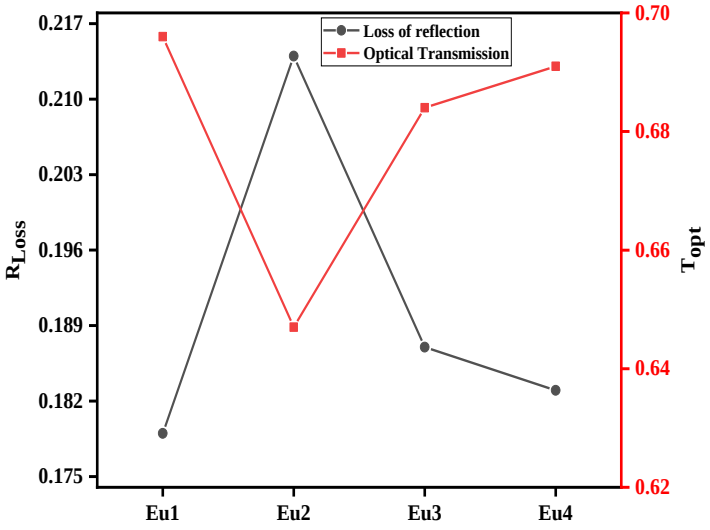

Fig.6. Dependence of R_{Loss} and T_{opt} on Eu_2O_3 content.

Conclusion

In conclusion, the optical properties of Eu_2O_3-doped borate glasses with the composition (45-x) B_2O_3-6PbO-18ZnO-31Bi_2O_3–xEu_2O_3 were systematically analyzed. UV-Vis absorption spectra revealed characteristic Eu_2O_3 transitions, with absorption intensities increasing as Eu_2O_3 content rose. Optical bandgap values initially decreased (Eu1 to Eu2) due to an increase in non-bridging oxygens (NBOs) and structural changes, followed by an increase (Eu3 to Eu4) as electron localization decreased. Trends in Urbach energy (E_U) highlighted variation in defect formation and structural rigidity, while changes in the refractive index (n) and dielectric constant (ε) were correlated with the NBO/BO ratio. Other optical parameters, such as molar refractivity (R_{Molar}) and polarizability (α_{Molar}), further confirmed these structural trends. The optical transmission and metallization values highlighted the dual impact of Eu_2O_3 on the glass network's metallic and non-metallic characteristics. These findings emphasize the significant influence of Eu_2O_3 content on the optical behavior and structural dynamics of the glass matrix, making it suitable for optoelectronic and photonic applications.

References

[1] L. Srinivasa Rao, S. Hussain, A. Navalika, B. Chennakesava Rao, T. Venkatappa Rao, F.C. Hila, Effect of ZnO nanoparticles on physical, optical and radiation shielding properties of Bi2O3-B2O3-Cr2O3 glasses, Progress in Results in Optics 12 (2023) 100491.

[2] K.M. Kaky, M.I. Sayyed, M.K. Hamad, S. Biradar, M.H.A. Mhareb, U. Altimari, M.M. Taki, Bismuth oxide effects on optical, structural, mechanical, and radiation shielding features of borosilicate glasses, Optical Materials 155 (2024) 115853.

[3] H. Karami, V. Zanganeh, M. Ahmadi, Study nuclear radiation shielding, mechanical and acoustical properties of TeO2-Na2O-BaO-TiO2 alloyed glasses, Progress in Radiation Physics and Chemistry 208 (2023) 110917.

[4] M.I. Sayyed, Modulation of optical, mechanical and radiation shielding characteristics in TeO2-B2O3–BaO–CeO2 glasses with varying CeO2 level, Optical Materials 158 (2025) 116492.

[5] R. Rajaramakrishna, W. Chaiphaksa, S. Kaewjaeng, S. Kothan, J. Kaewkhao, Study of radiation shielding and luminescence properties of 1.5 μm emission from Er3+ doped zinc yttrium borate glasses, Progress in Optik - International Journal for Light and Electron Optics 289 (2023) 171273.

[6] B. Aktas, A. Acikgoz, D. Yilmaz, S. Yalcin, K. Dogru, N. Yorulmaz, The role of TeO2 insertion on the radiation shielding, structural and physical properties of borosilicate glasses, Progress in Journal of Nuclear Materials 563 (2022) 153619.

[7] J. Singh, P. Kaur, P. Kaur, V. Kumar, M.S. Al-Buriahi, N. Alfryyan, Z.A. Alrowaili, T. Singh, Optical and radiation shielding features for some phospho-silicate glasses, Progress in Optik - International Journal for Light and Electron Optics 261 (2022) 169140.

[8] B. Guven, E. Ercenk, S. Yilmaz, Investigation of radiation shielding properties of basalt-based glasses: Binodal / Spinodal decomposition effect theory, Progress in Nuclear Energy 163 (2023) 104810.

[9] M. Elsafi, A.M. Hedaya, E.H. Abdel-Gawad, M. Rashad, M.I. Sayyed, I.H. Saleh, Experimental investigation of the radiation shielding performance of a newly developed silicon epoxy resin doped with WO3 micro/nanoparticles, Silicon.

[10] Z.M. Cinan, Innovative phosphate glasses of advanced material designs for radiation shielding, Nexus of Future Materials 1 (2024) 92-101.

[11] E.L. Ruiz, Radiation shielding analysis of barium-titanium-borate glasses doped with zinc oxide, Nexus of Future Materials 1 (2024) 80-85.

[12] M.H. Pacheco, M.S. Gibin, M.A. Silva, G. Montagnini, R.C. Viscovini, A. Steimacher, F. Pedrochi, V.S. Zanuto, R.F. Muniz, BaO–reinforced SiO2–Na2O–Ca(O/F2)–Al2O3 glasses for radiation safety: On the physical, optical, structural and radiation shielding properties, Progress in Journal of Alloys and Compounds 960 (2023) 171019.

[13] J. Wu, J. Hu, Z. Deng, Y. Feng, H. Fan, Z. Wang, K. Wang, Q. Chen, W. Zhang, Comparative investigation of physical, X-ray and neutron radiation shielding properties for B2O3-MnO2-CdO borate glasses, Progress in Ceramics International 49 (2023) 30915–30923.

[14] J. Alyami, Y. Al-Hadeethi, O.A. Fallatah, S. Biradar, M.I. Sayyed, F. Almutairi, Tailoring glass characteristics: Unveiling the impact of PbO and ZnO in titanium-barium borate glasses for advanced radiation protection, Annals of Nuclear Energy 212 (2025) 111069.

[15] M. Fidan, A. Acikgoz, G. Demircan, D. Yilmaz, B. Aktas, Optical, structural, physical, and nuclear shielding properties, and albedo parameters of TeO2–BaO–B2O3–PbO–V2O5 glasses, Journal of Physics and Chemistry of Solids 163 (2022) 110543.

[16] M.I. Sayyed, A.H. Almuqrin, C.V. More, U. Rilwan, M. Rashad, M. Elsafi, Exploring gamma radiation shielding: the role of BaO in borosilicate glasses, Silicon.

[17] M.I. Sayyed, U. Rilwan, K.A. Mahmoud, M. Elsafi, Experimental study of the radiation shielding characteristics of new PbO–Na2O–B2O3–BaO glasses, Nuclear Engineering and Technology 56 (2024) 2437-2443.

[18] M.A. Sayed, B. Basha, N. Al-Harbi, A.M. Al-Baradi, K.S. Shaaban, PbO effect on physical, mechanical, optical, structural, and radiation characteristics of P2O5-BaO-PbO glass system, The European Physical Journal Plus 138 (2023) 455.

[19] A.H. Almuqrin, K.A. Mahmoud, U. Rilwan, M.I. Sayyed, Influence of various metal oxides (PbO, Fe2O3, MgO, and Al2O3) on the mechanical properties and γ-ray attenuation performance of zinc barium borate glasses, Nuclear Engineering and Technology 56 (2024) 2711-2717.

[20] H. Eskalen, Y. Kavun, M. Kavgacı, Preparation and study of radiation shielding features of ZnO nanoparticles reinforced borate glasses, Progress in Applied Radiation and Isotopes 198 (2023) 110858.

[21] Ö. Akçalı, M. Çağlar, O. Toker, B. Bilmez, H.B. Kavanoz, O. Içelli, An investigation on gamma-ray shielding properties of quaternary glassy composite (Na2Si3O7/Bi2O3/B2O3/Sb2O3) by BXCOM and MCNP 6.2 code, Progress in Nuclear Energy 103364 (2020).

[22] S. Biradar, M.N. Chandrashekara, A. Dinkar, G.B. Devidas, A.S. Bennal, R. Rajaramakrishna, M.I. Sayyed, Synergistic optimization of physical, thermal, structural, mechanical, optical and radiation shielding characteristics in borate glasses doped with Bi2O3, Optical Materials 155 (2024) 115815.

[23] K.M. Kaky, M.I. Sayyed, K.A. Mahmoud, M.H.A. Mhareb, S. Biradar, A.J. Kadhim, A comprehensive investigation on lanthanum ions doped borate-tellurite-germinate glass for radiation shielding and optical application, Progress in Nuclear Energy 176 (2024) 105402.

[24] S. Biradar, A. Dinkar, G.B. Devidas, A comprehensive study of the effect of BaO doping on the physical, mechanical, optical, and radiation shielding properties of borate-based glasses, Nexus of Future Materials 1 (2024) 108-119.

[25] M.I. Sayyed, M.J. Zaiter, M.H.A. Mhareb, K.A. Mahmoud, S. Biradar, R.I. Mahdi, K.M. Kaky, Optical, physical, mechanical, structural, and radiation shielding investigations of B2O3–TeO2-GeO2-MgO-PbO for ionizing protection and optical transmission application, Optical Materials 154 (2024) 115807.

[26] S. Biradar, M.N. Chandrashekara, A. Dinkar, G.B. Devidas, A.S. Bennal, M.I. Sayyed, E. Es-soufi, A multifaceted study of B2O3-BaO-PbO-WO3 glasses doped with Bi2O3: Insights from physical, thermal, structural, mechanical and optical analyses towards improved shielding properties, Ceramics International.

[27] M.I. Sayyed, S. Biradar, T.A. Maghrbi, Y. Faruque, M.R.I. Abdullah, S. Yasmin, Optimization of optical properties and radiation shielding efficiency in BaO-PbO2-B2O3-Dy2O3 glass systems, Optical Materials.

[28] J. Rajagukguk, J. Kaewkhao, M. Djamal, R. Hidayat, Y. Ruangtaweep, Structural and optical characteristics of Eu3+ ions in sodium-lead-zinc-lithium-borate glass system, Journal of Molecular Structure 1121 (2016) 180-187.

[29] P. Krishnapuram, S.K. Jakka, C. Thummala, R.M. Lalapeta, Photoluminescence characteristics of Eu2O3 doped calcium fluoroborate glasses, Journal of Molecular Structure 1028 (2012) 170-175.

[30] S. Biradar, A. Dinkar, A.S. Bennal, G.B. Devidas, B.T. Hareesh, M.K. Siri, M.N. Chandrashekara, Comprehensive investigation of borate-based glasses doped with BaO: An assessment of physical, structural, thermal, optical, and radiation shielding properties, Optical Materials 150 (2024) 115176.